Effect of the morphological characteristics and size distribution on the rheological properties of Cellulose Nanofibrils dispersions

Gregory Albornoz-Palma, Daniel Ching, and Miguel Pereira

Department of Chemical Engineering
Engineering Faculty
Universidad de Concepción

TAPPI Nano 2021 Virtual Conference
15-16 June 2021

TAPPI NANO DIVISION

Adapted from Albornoz-Palma et al., (2020)

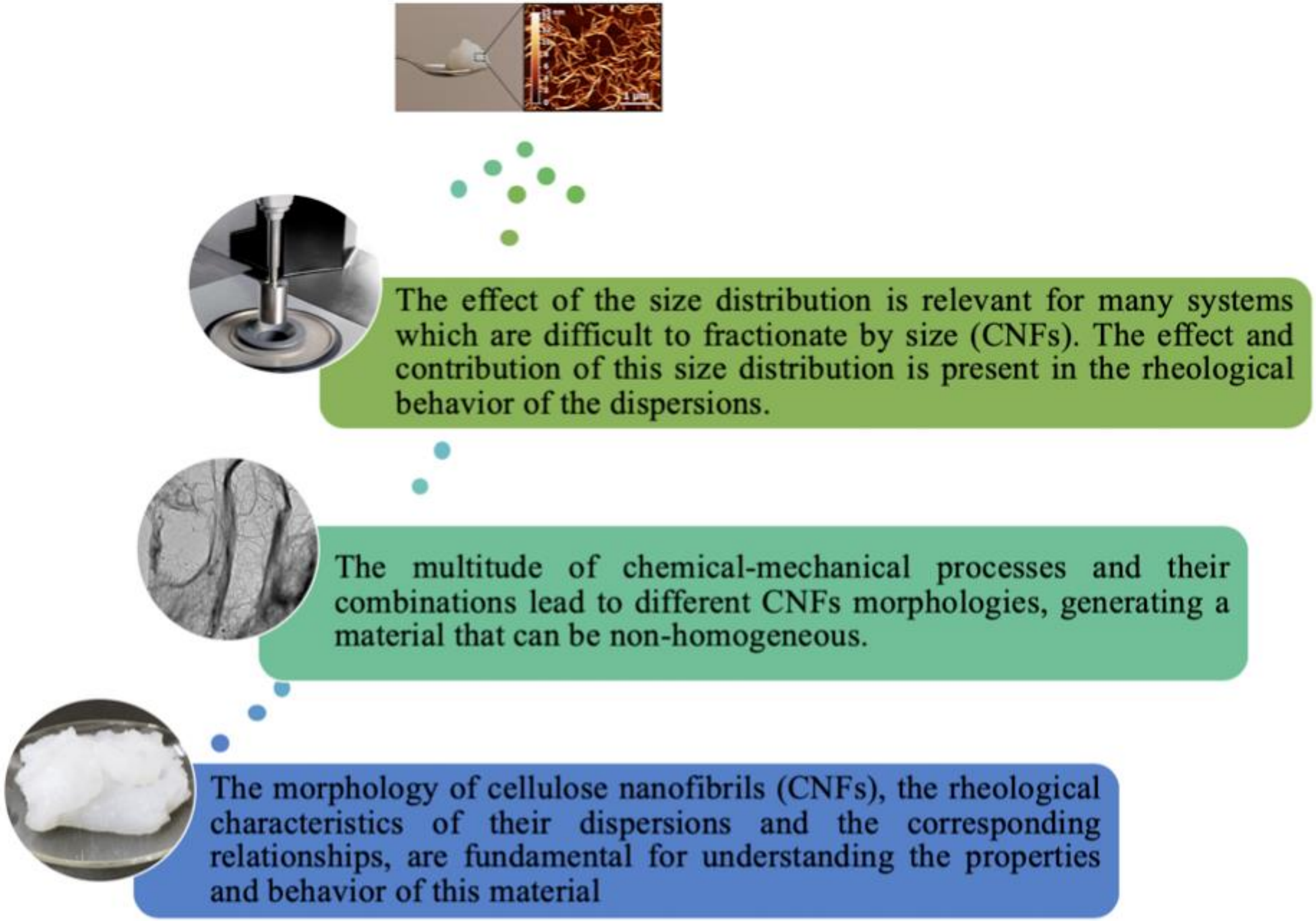

Goals

Understanding how the morphological characteristics of the CNFs produced by enzymatic treatment and their fractionation by size affect the rheological behavior of the dispersions in the dilute and semi-concentrated region.

Understanding the contribution of the different sized fractions on the resulting rheological properties and establish relationships between both properties.

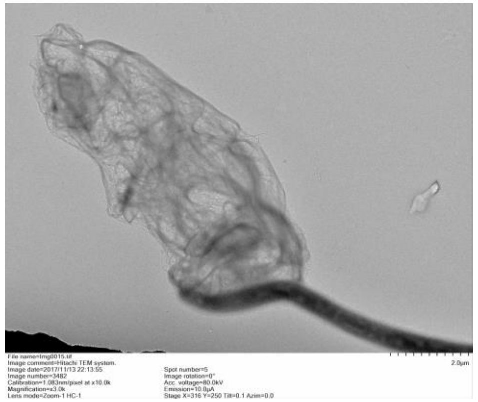

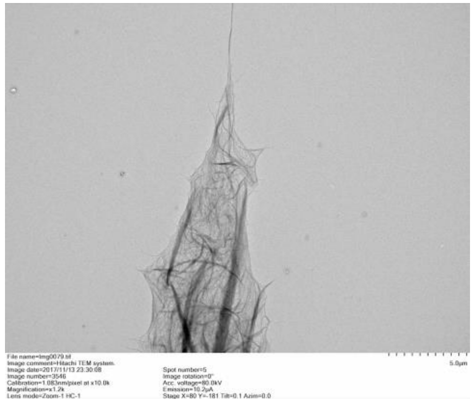

Background

Cellulose nanofibrils refers to fibrils with nanoscale side dimensions (< 100 nm) whose average lengths are believed to be in the order of several micrometers

Cellulose nanofibrils are high aspect ratio nano-objects (semi-flexible) that are obtained from the cell walls of wood fibers and plants through different mechanical, enzymatic and/or chemical processes

The different methods for obtaining CNFs and their combinations lead to different morphological and surface properties, as well as different rheological behavior.

Fibrillation produces a material that may be nonhomogeneous, containing fibers, fiber fragments, fines and fibrils

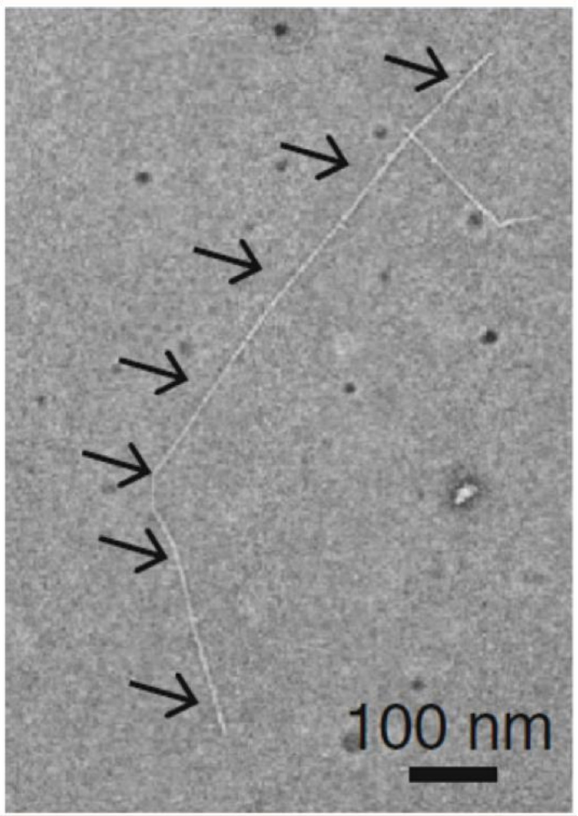

Cellulose nanofibers (Tanaka et al., 2014)

Background

Cellulose nanofibrils refers to fibrils with nanoscale side dimensions (< 100 nm) whose average lengths are believed to be in the order of several micrometers

Cellulose nanofibrils are high aspect ratio nano-objects (semi-flexible) that are obtained from the cell walls of wood fibers and plants through different mechanical, enzymatic and/or chemical processes

The different methods for obtaining CNFs and their combinations lead to different morphological and surface properties, as well as different rheological behavior.

Fibrillation produces a material that may be nonhomogeneous, containing fibers, fiber fragments, fines and fibrils

TEMPO-oxidized CNF dispersions at 1% (w/w)

Enzymatic CNF dispersions at 1% (w/w)

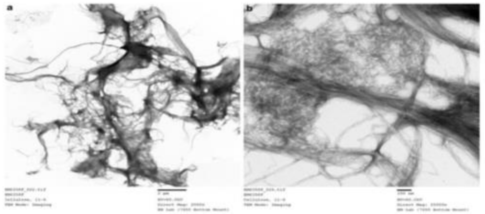

TEM micrographs of CNFs (Wang et al., 2012)

Background

Rheology of CNF dispersions

Regardless of the production conditions and above a critical concentration, CNF dispersions have the following characteristics:

- Shear thinning behavior (pseudoplastic fluid)
- Thixotropic
- Once the shear rate is reduced to zero, the viscosity of the dispersion increases to its resting value

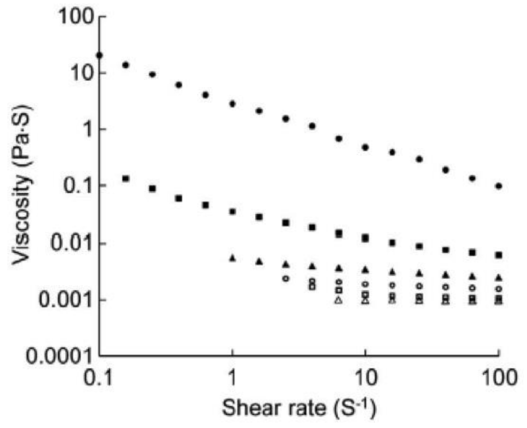

Viscosity depending on the shear rate
(Iwamoto et al., 2014)

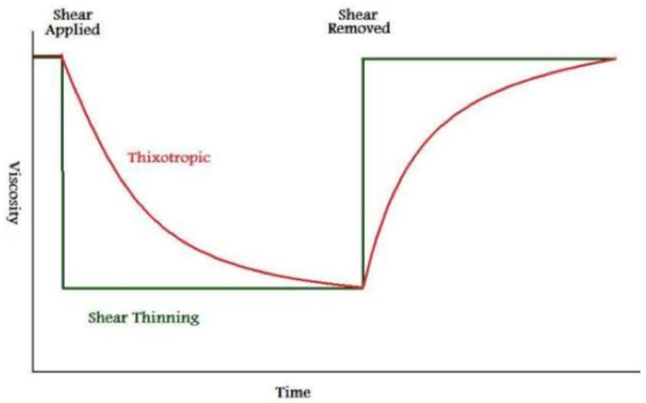

Thixotropic behavior

Background

Rheology of CNF dispersions

Shear viscosity is dependent on the type of CNFs, solvent, aspect ratio, temperature, concentration, and pH

Fibrillation intensity	Concentration	Temperature	pH

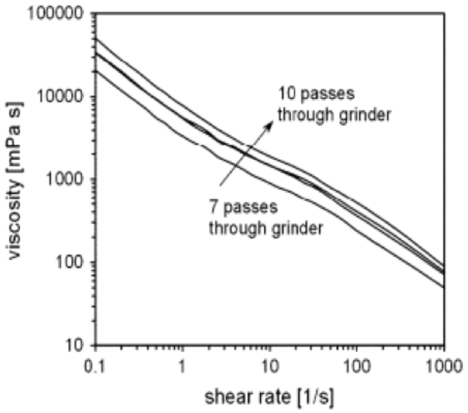

Grüneberger et al., (2014)

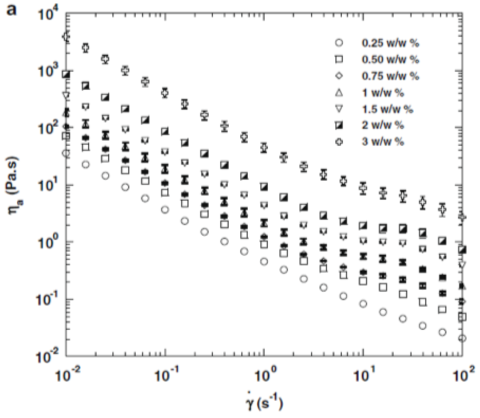

Agoda-Tandjawa et al., (2010)

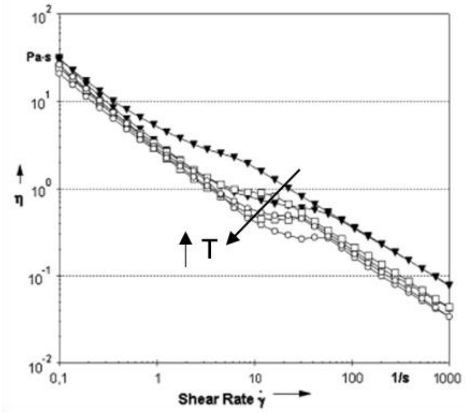

Iotti et al., (2011)

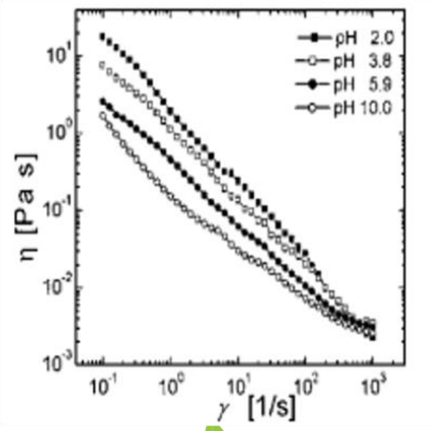

Pääkkö et al., (2007)

Viscosity-concentration relation

The dispersion viscosity is dependent of the concentration, and generally three regions can be distinguished:

- Dilute region: interaction effects are not significant (Newtonian viscosity).
- Concentrated region: viscosity shear rate dependent due to entanglement. Effect of concentration is stronger.
- Semi-dilute or semi-concentrated region: particle chain start to entangle and aggregate. Determined by aspect ratio, temperature, and concentration.

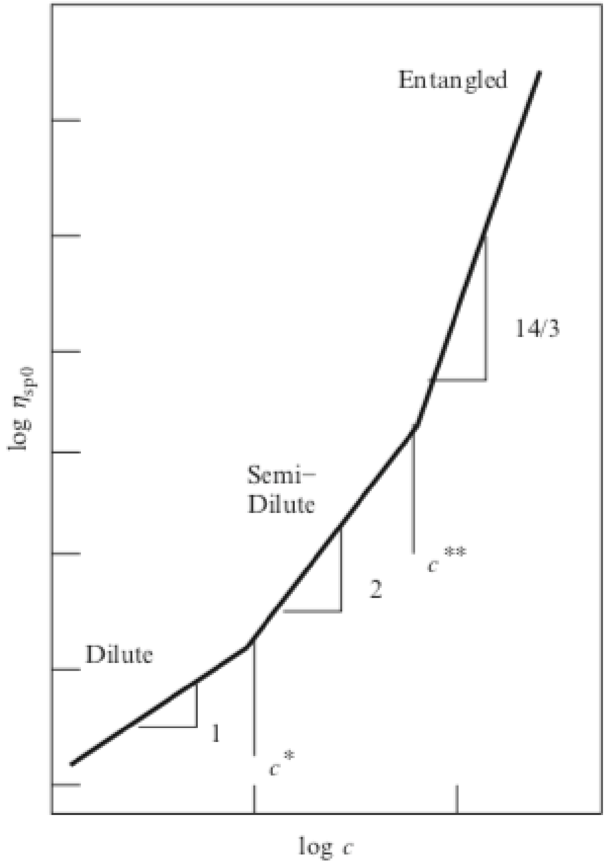

Background

Viscosity-concentration relation

The dispersion viscosity is dependent of the concentration, and generally three regions can be distinguished:

- Dilute region: interaction effects are not significant (Newtonian viscosity).
- Concentrated region: viscosity shear rate dependent due to entanglement. Effect of concentration is stronger.
- Semi-dilute or semi-concentrated region: particle chain start to entangle and aggregate. Determined by aspect ratio, temperature, and concentration.

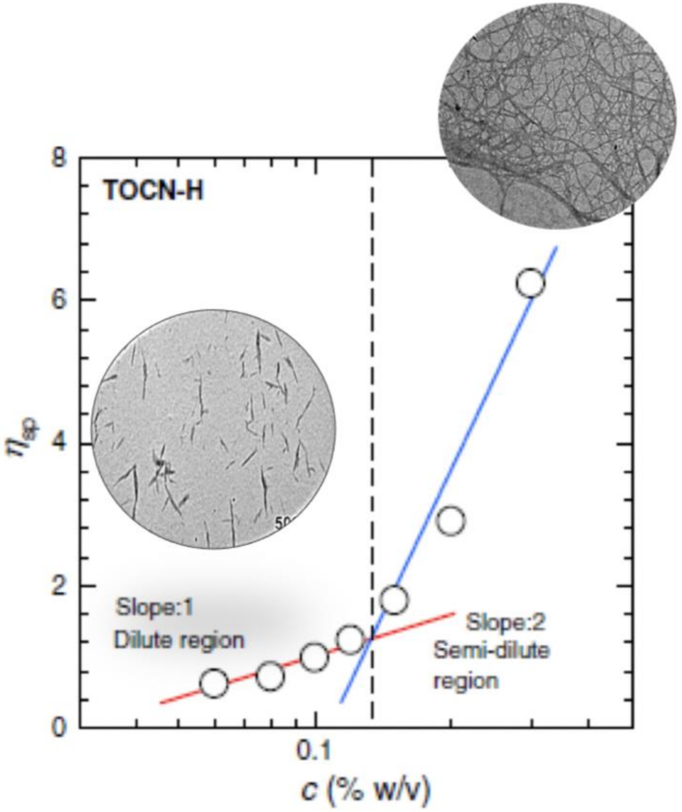

Specific viscosity of nanocellulose dispersions (Tanaka et al., 2014)

Background

Size distribution

Polydispersity (size)

On polydisperse systems, more than one size is present. The effect on the virial expansion is additive:

$$\eta = \eta_0(1 + \sum_i [\eta]_i c_i)$$

It follows that the intrinsic viscosity of a dispersion containing a distribution of size is given by

$$[\eta] = \sum_i [\eta]_i x_i \qquad (1)$$

where x_i is mass fraction of each species i (Mansfield y Douglas, 2008a).

Nonideal mixing behavior of the dispersion

The mixing rule used to calculate the viscosity of mixtures from viscosities of components is the so-called ideal linear mixture with the introduction of a non-linear term:

$$\eta = \sum_i x_i \eta_i + \Delta\eta \qquad (2)$$

Materials and methods

Material:

The raw material for the production of CNF dispersions was bleached hardwood kraft pulp supplied by CMPC Pulp S.A. Chile.

Preparation of CNF dispersions:

Seven CNF samples were prepared with enzymatic pretreatment (Maximyze 2566 enzyme at 1.2%) and disintegration of the fiber suspension through different numbers of passes in a GEA Niro Soavi homogenizer at a concentration of 0.5% (w/w).

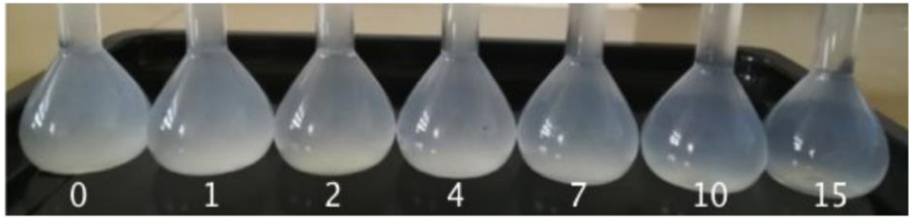

Materials and methods

Shear viscosity measurement:

To determine the dynamic viscosity of the different CNF dispersions, a Brookfield LVDV-I+ viscometer was used with a configuration of double-cylinder geometry (cup radius: 1.37 cm; spindle radius: 1.25 cm).

The measurement conditions were:

- Temperature of 23ºC
- Shear rate of 73.38s^{-1}.

Length of the CNFs:

The length distribution was determined experimentally using an S3500 Laser Diffraction Particle Size Analyzer (Microtrac Inc. USA).

Materials and methods

Width of the CNFs:

The width distribution of the CNFs was obtained by simple random sampling, using micrographs of transmission electron microscopy (Hitachi TEM) at different scales (magnification: x2.5k, x8.0k, x15.0k, and x25.0k).

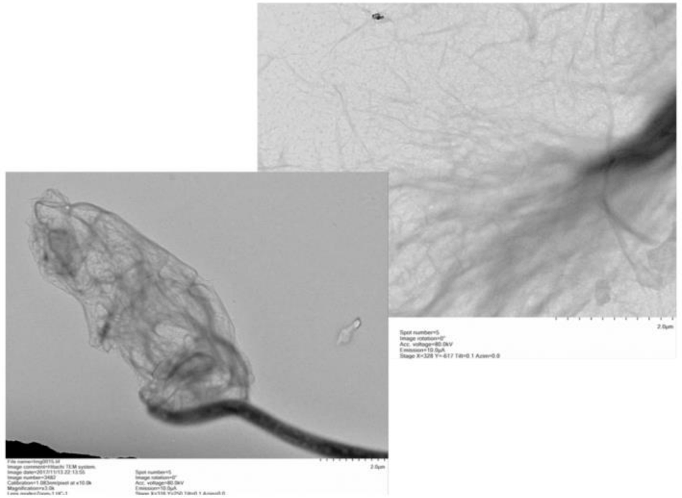

Fractionation by size:

For the fractionation of the samples, the dispersions were passed through different meshes using the Williams Precision Freeness Tester filtration system, with meshes of 45, 60, 100, 200, and 400.

Results and discussion

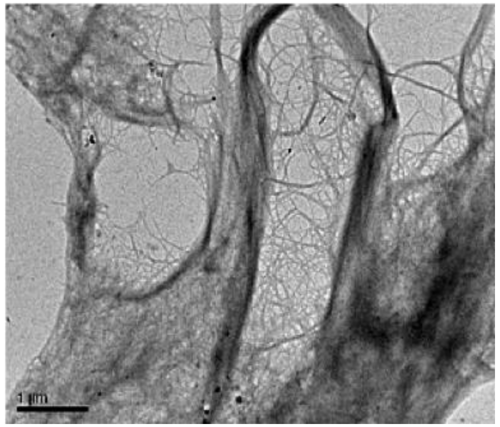

0 passes

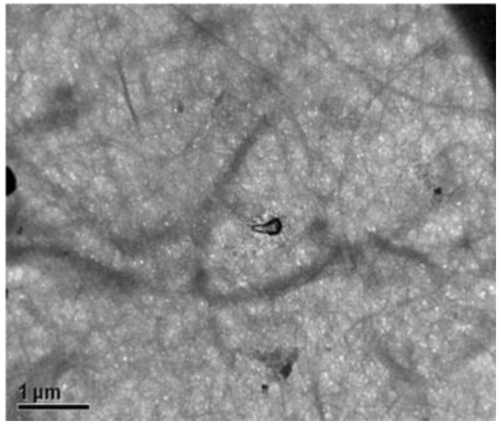

1 pass

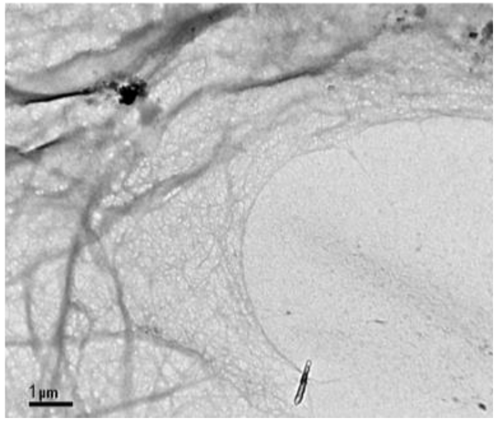

2 passes

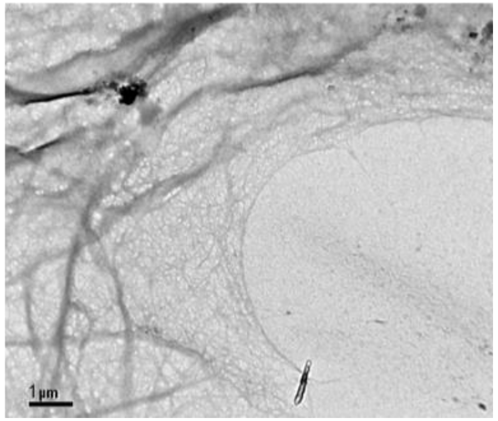

4 passes

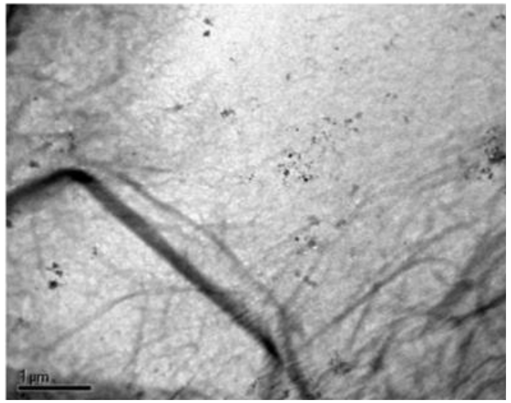

7 passes

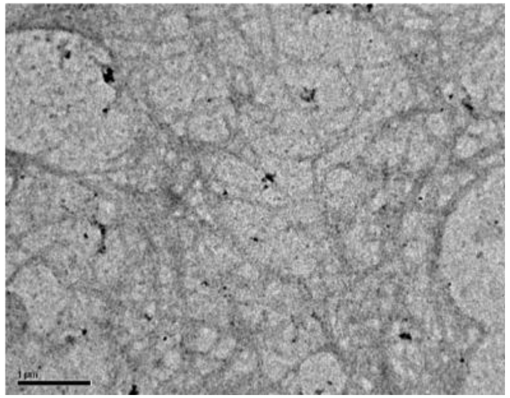

10 passes

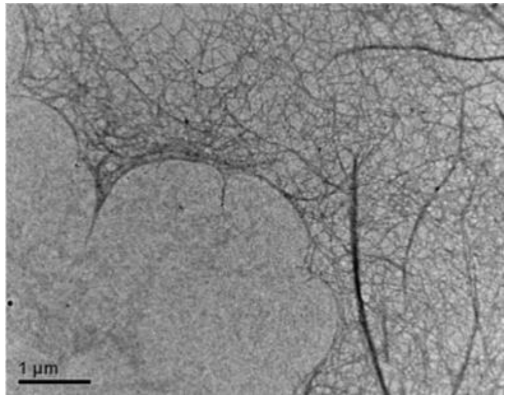

15 passes

Results and discussion

Width distribution of CNF

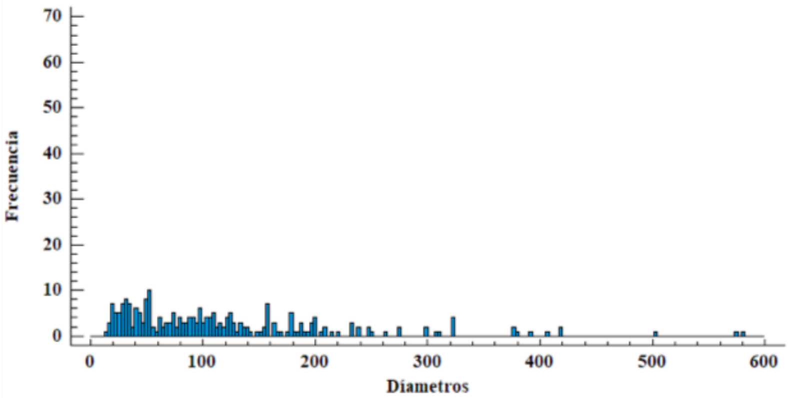

0 passes

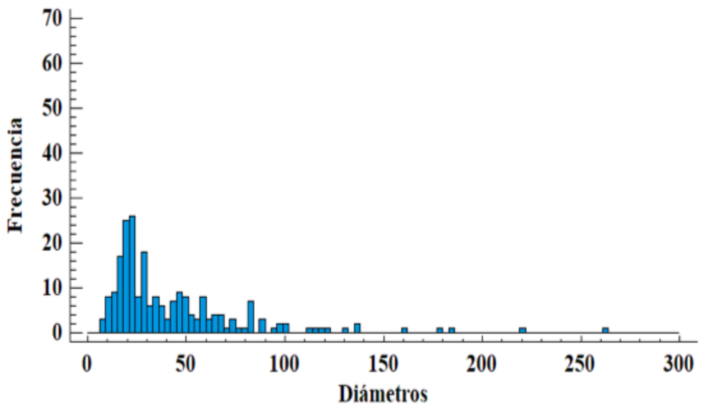

1 pass

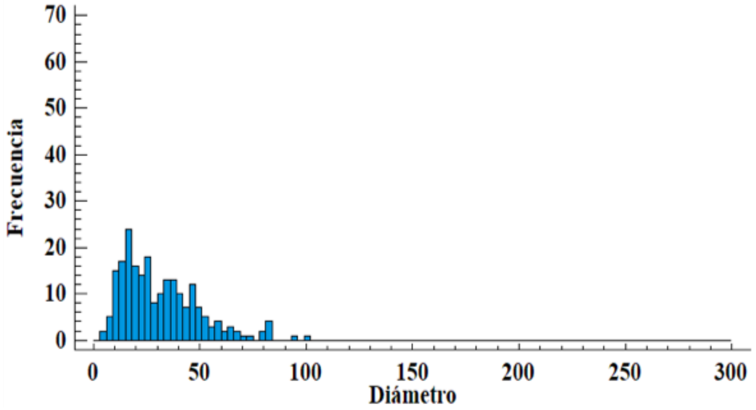

2 passes

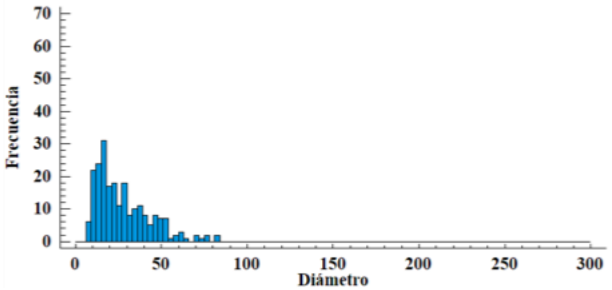

4 passes

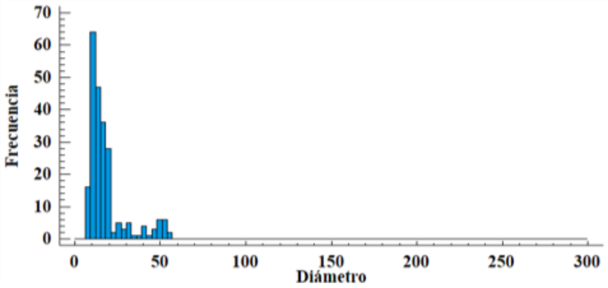

7 passes

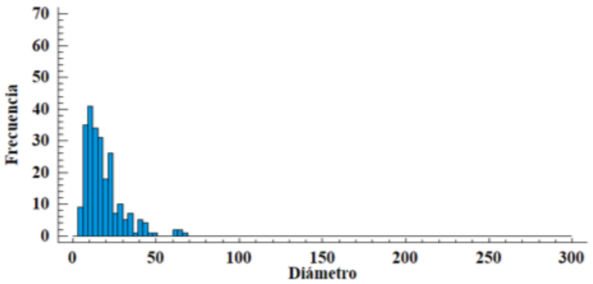

10 passes

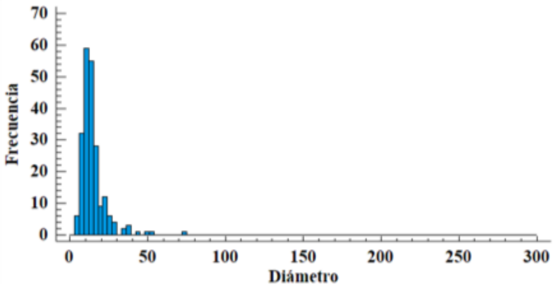

15 passes

Results and discussion

Length distribution of CNF

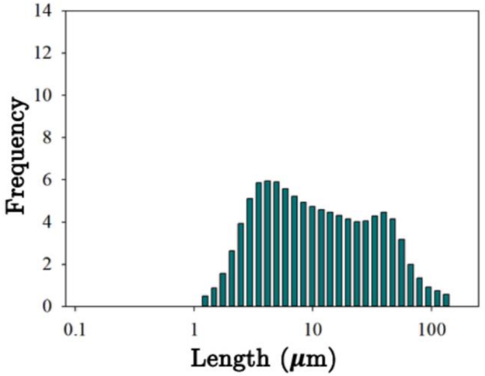

0 passes

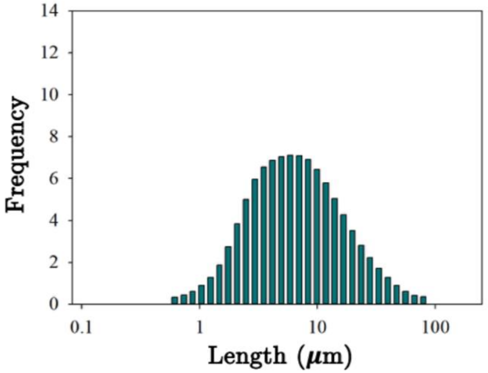

1 pass

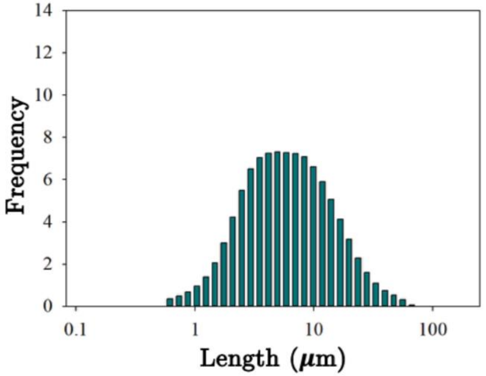

2 passes

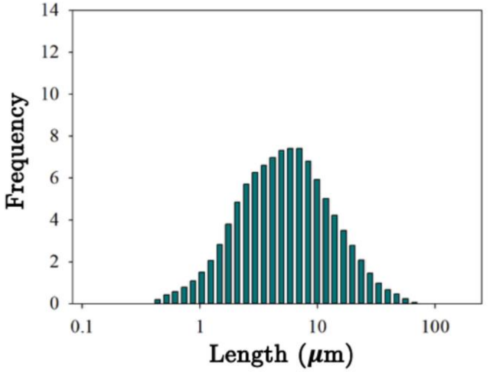

4 passes

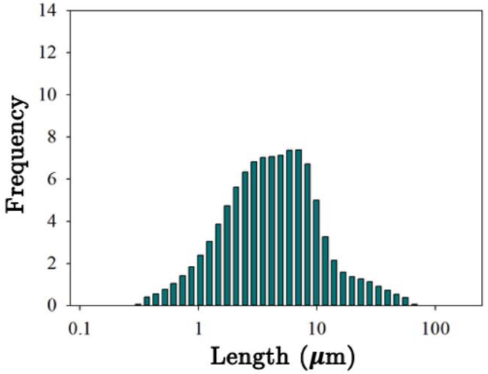

7 passes

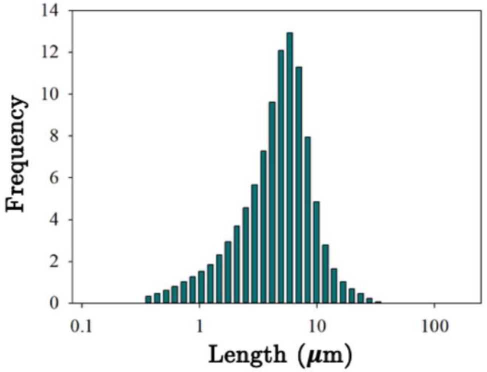

10 passes

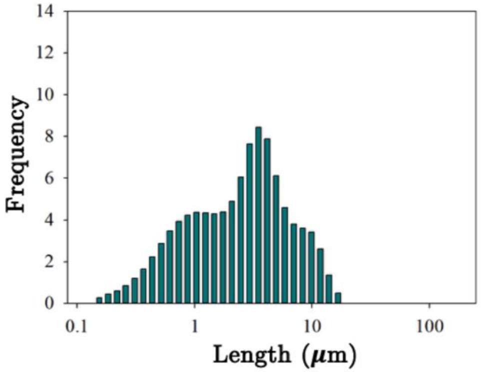

15 passes

Results and discussion

Morphological and rheological characteristics of CNF

Nº	Average width \nm	S.D. of the sample[(a)] \nm	Homogeneous groups[(b)]	Average length \µm	S.D. of the sample \µm	Homogeneous groups[(b)]	Aspect ratio	Critical concentration \g/ml	Intrinsic viscosity \ml/g
0P	121.4±1.0	68.1	A	17.7±0.4	15.9	A	145.5	0.00238	323.2
1P	42.6±0.4	22.3	B	8.9±0.4	6.3	B	210.1	0.00156	684.4
2P	31.6±0.2	13.0	C	7.7±0.4	5.3	C	243.8	0.00107	801.6
4P	28.2±0.2	10.6	D	7.5±0.2	5.3	C	264.8	0.00097	885.2
7P	18.2±0.2	6.3	E	5.9±0.3	3.7	D	325.4	0.00063	1481.6
10P	18.1±0.3	6.0	E	5.0±0.4	3.5	E	278.7	0.00085	1102.5
15P	14.6±0.1	4.0	F	4.4±0.8	3.3	E	304.6	0.00066	1339.8

[(a)]Normal distribution by central limit theorem

[(b)]Test of Multiple Range: Method of Duncan

Results and discussion

Wormlike chain model

Wormlike chain model provides a reasonable representation of semi-flexible particles. This model allows a determination of the intrinsic viscosity of macromolecules, nanoparticles and essentially any arbitrary shaped particle.

Parameters:

$$\varepsilon = \frac{a}{L}$$

where a is the persistent length and L is the total length of the chain's contour; and

$$\delta = \frac{d}{L} = \frac{1}{p}$$

where d corresponds to the width of the chain.

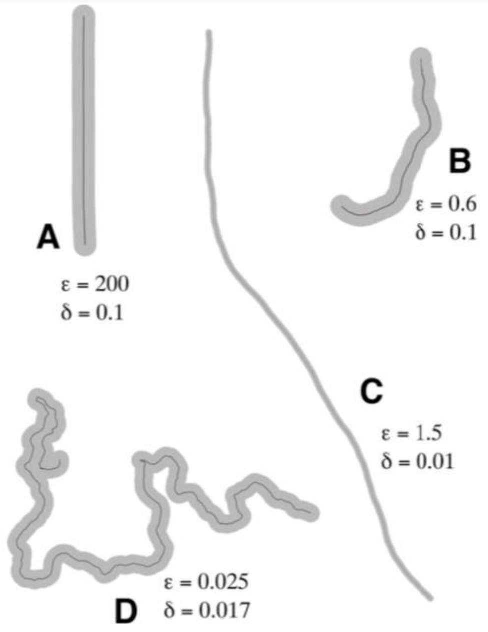

Aspect ratio and flexibility of wormlike chain based on δ and ε (Mansfield y Douglas, 2008b).

Results and discussion

Wormlike chain model

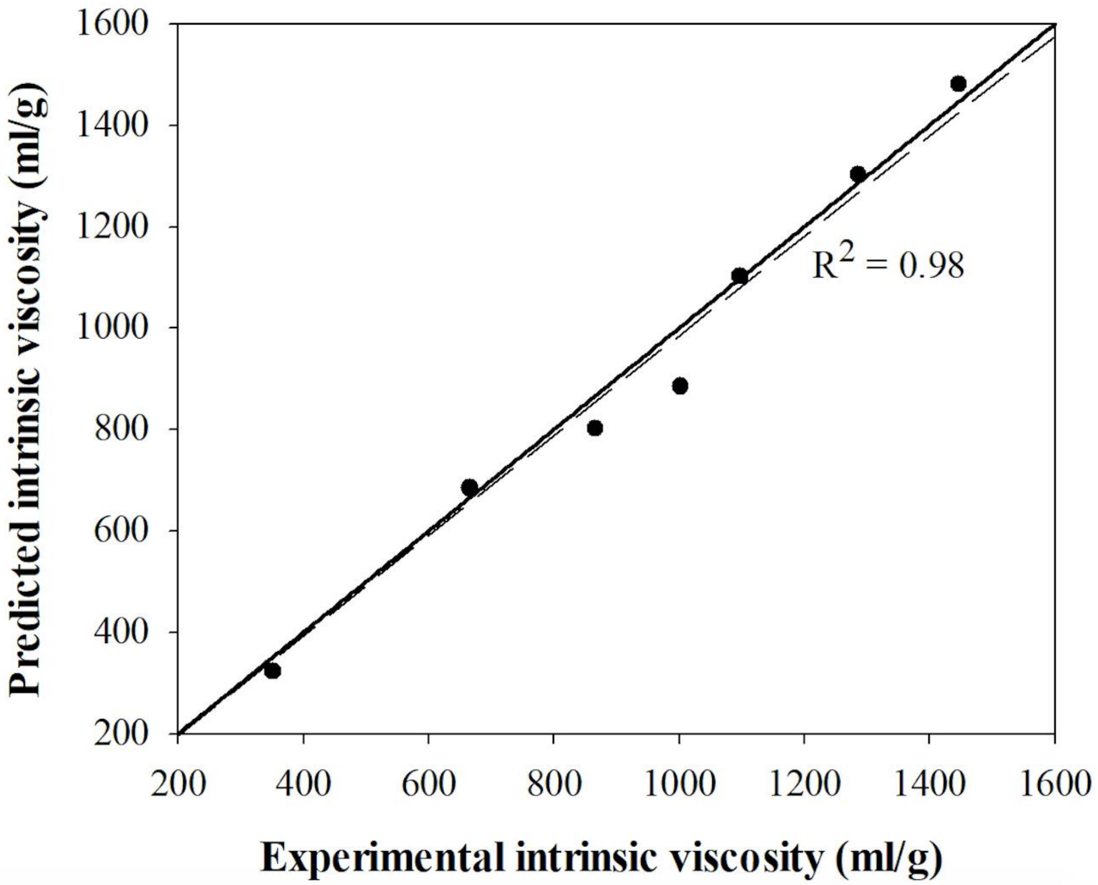

Equation:

$$[\eta]_{predicted} = 1.01[\eta]_{experimental}$$

Results and discussion

Relationship between intrinsic viscosity and aspect ratio of CNFs

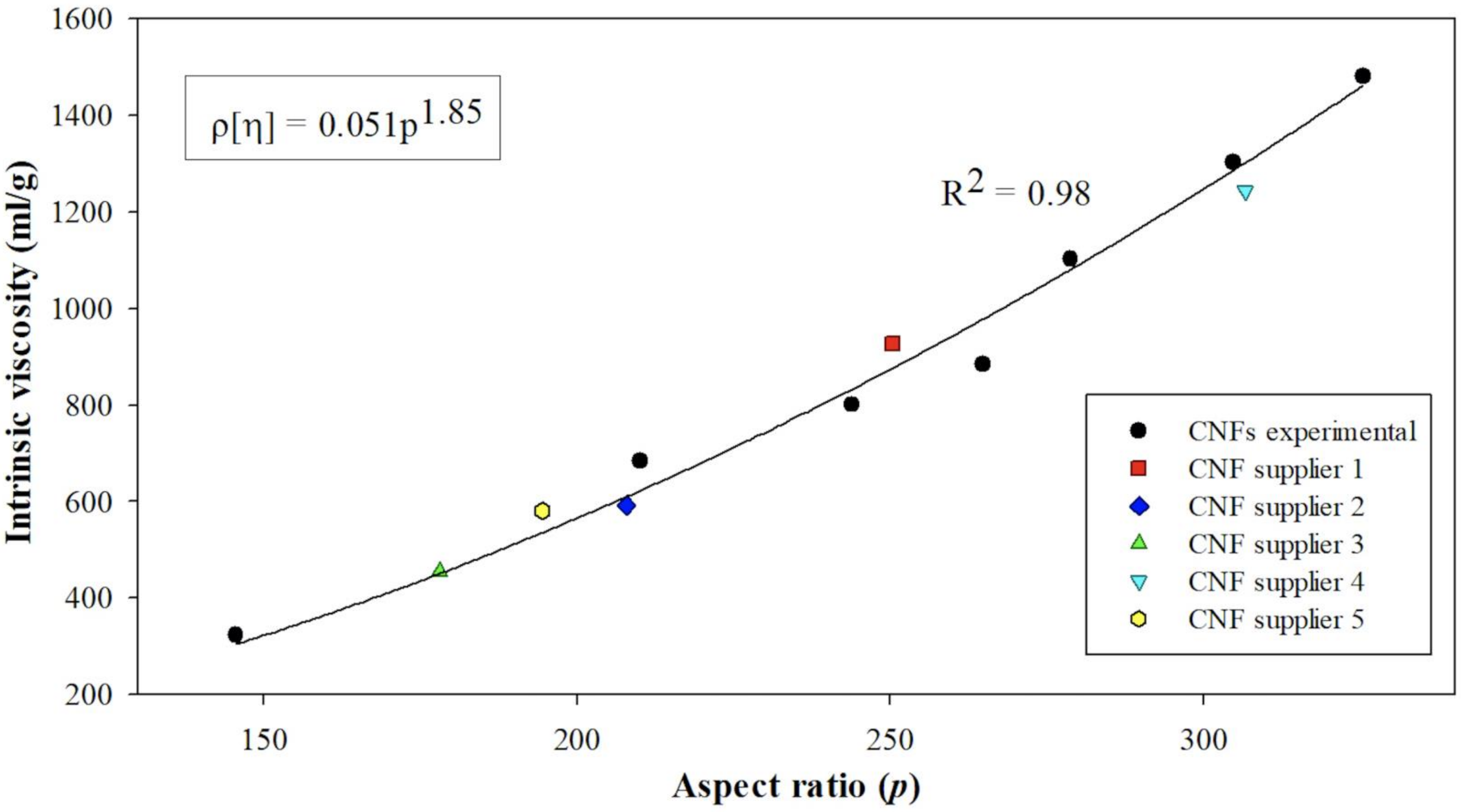

Equation:

$$\rho[\eta] = 0.051p^{1.85}$$

Results and discussion

Size distributions

To study the effects generated by the size distribution in the rheological properties of each sample in the diluted and semi-concentrated region, different mass fractions were separated

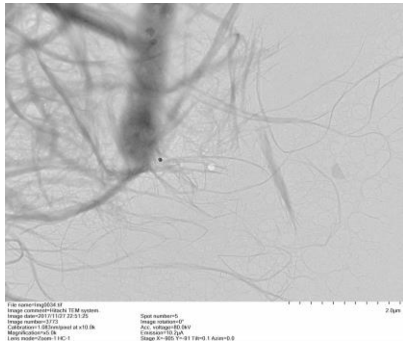

Fraction 1

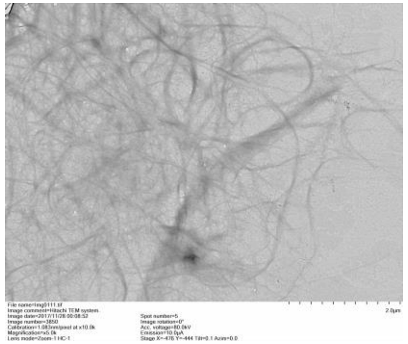

Fraction 2

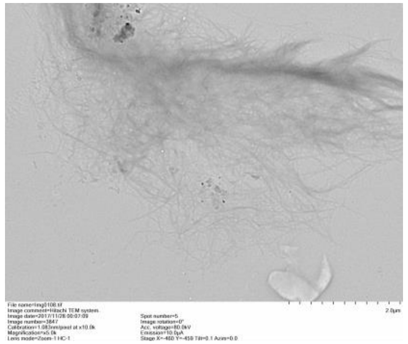

Fraction 3

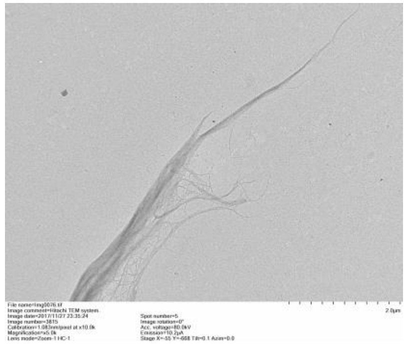

Fraction 4

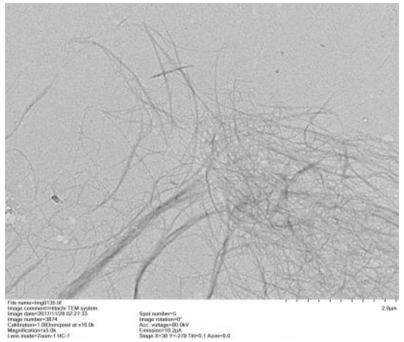

Fraction 5

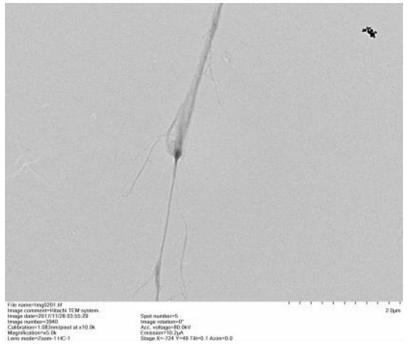

Fraction 6

Results and discussion

Fractionation by size

Fraction	0 passes	1 pass	2 passes	4 passes	7 passes	10 passes	15 passes
1	36.6%	2.3%	-	-	-	-	-
2	37.0%	4.3%	0.6%	-	-	-	-
3	7.0%	6.1%	2.1%	0.7%	0.1%	-	-
4	6.4%	8.7%	5.2%	2.1%	0.4%	0.4%	0.2%
5	3.4%	18.0%	14.2%	11.3%	12.0%	11.3%	1.9%
6	9.6%	60.6%	77.9%	85.9%	87.5%	88.3%	97.9%

Results and discussion

Morphological and rheological characteristics of fractions

Fraction	Average width \nm	S.D. of the sample[a] \nm (Coefficient of variation \%)	Average length \μm	S.D. of the sample \μm (Coefficient of variation \%)	Aspect ratio	Critical concentration \g/ml	Intrinsic viscosity \g/ml
1	180.1±0.5	64.6(36)	16.9±0.4	10.2(60)	93.6	0.0076[b]	134.0
2	100.8±0.5	47.7(47)	15.9±0.5	9.5(60)	158.0	0.0023	356.9
3	84.3±0.4	30.8(37)	15.8±0.1	8.6(54)	187.9	0.0021	502.2
4	56.1±0.3	26.2(47)	12.1±0.7	7.2(59)	214.9	0.0016	596.0
5	44.9±0.3	19.6(44)	10.4±0.5	5.1(49)	230.8	0.0011	786.6
6, 0 passes	28.3±0.2	12.7(45)	6.7±0.1	3.4(51)	237.2	0.0010	807.7
6, 7 passes	16.1±0.3	7.2(45)	5.2±0.3	2.3(44)	323.7	0.00057	1567.9
6, 15 passes	13.1±0.2	3.4(26)	4.0±0.3	2.0(50)	306.2	0.00062	1361.5

[a]Normal distribution by the central limit theorem.
[b]Calculated by equation $c^* = 67(1/p^2)$ (Albornoz-Palma *et al*., 2020)

Results and discussion

Fractionation by size

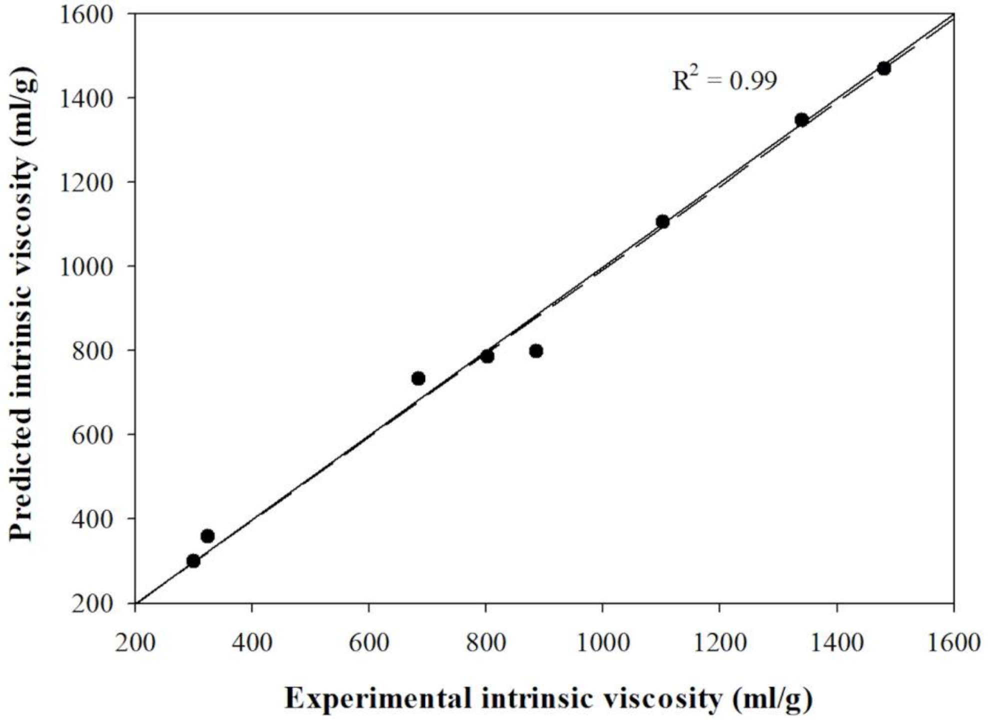

$$[\eta] = \sum_i [\eta]_i x_i$$

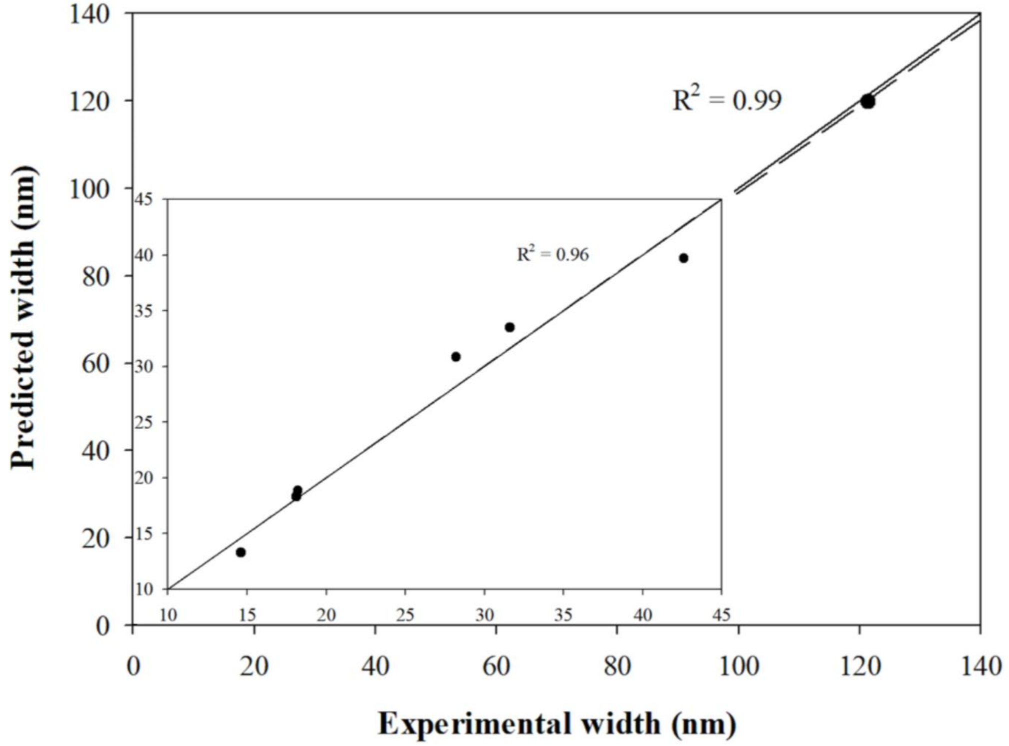

$$\bar{d} = \sum_i \bar{d}_i x_i$$

Results and discussion

Semi-concentrated region

In the semi-concentrated region the analysis can be difficult, due the viscosity of the samples depending on more factors

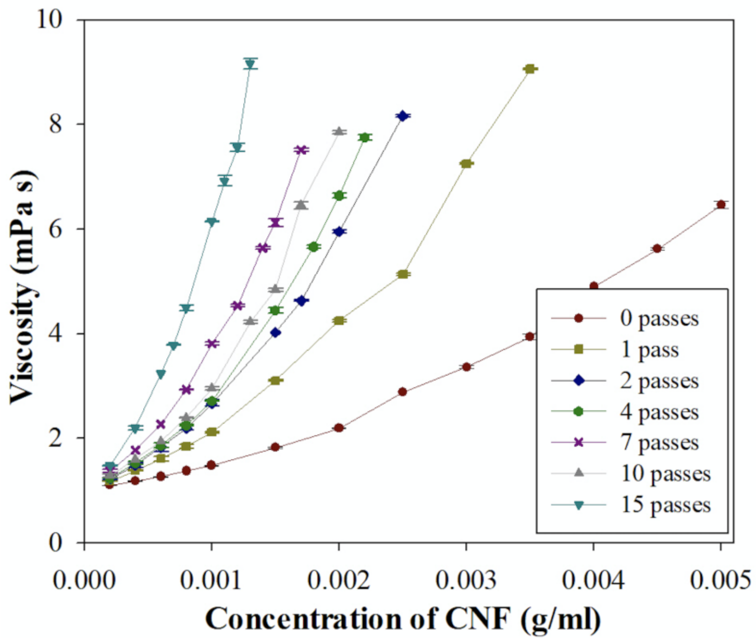

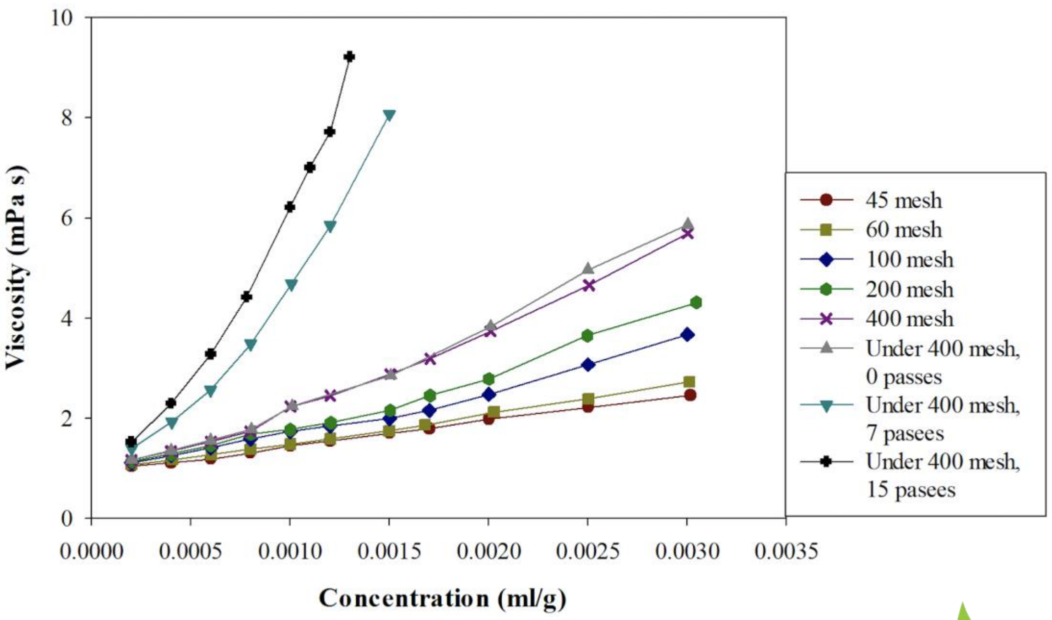

Results and discussion

Viscosity model (variables)

To study the contribution and synergy of the different parameters of relevance in the viscosity of each sample, a regression analysis was performed with 2 interactions.

The equation of the fitted model is ($p < 0.05$):

$$\eta = \eta_0 + a_1 * c + a_2 * L + a_3 * p + a_4 * c * p + a_5 * L * p$$

Statistic parameters:
R-squared = 91.4%
Dubin-Watson statistic = 1.7 (p = 0.06)

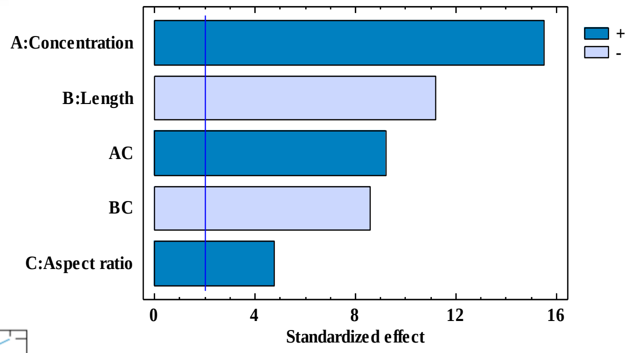

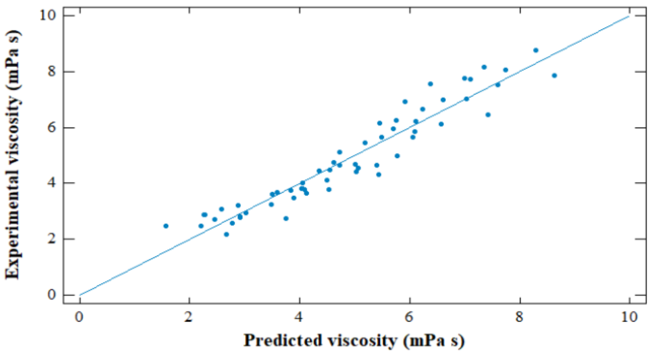

Results and discussion

Viscosity model (size distribution)

The model is:

$$\eta = \sum_i x_i \eta_i + \Delta\eta = \sum_i x_i \eta_i + \sum_{\substack{j,k \\ j>k}} x_j x_k \left(\frac{\eta_j + \eta_k}{2}\right) k_{jk} \begin{cases} k_{jk} = 0 \; dilute\ region \\ k_{jk} \neq 0 \; semi-dilute\ region \end{cases}$$

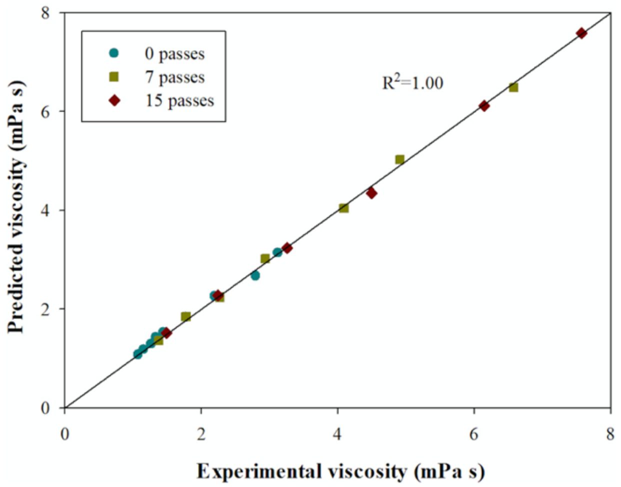

Interaction parameter

Interactions	1-2	2-3	3-4	4-5	5-6
0P	-0.310	-0.069	-0.015	-0.009	-0.015
7P	-	-	-	-0.002	-0.904
15P	-	-	-	-	-0.149

Conclusions

There is a strong relationship between the intrinsic viscosity of the CNF dispersions and their aspect ratio, which can be correlated by a power law model. Such model is independent of the flexibility of the CNFs.

In dilute region, the behavior of intrinsic viscosity of the samples is linear.

Regarding the degree of fibrillation, the morphology resulting from CNF distributions satisfactorily explains the viscosity of the CNF dispersions, which are explained by combined effects of CNF morphology through their fractions.

Acknowledgments

This work was funded by the Agencia Nacional de Investigación y Desarrollo (ANID)/Doctorado Nacional/2018–21181080 and Agencia Nacional de Investigación y Desarrollo (ANID)/Doctorado Nacional/2019–21190348.

References

- Agoda-Tandjawa, G., Durand, S., Berot, S., Blassel, C., Gaillard, C., Garnier, C.,& Doublier, J. L. (2010). Rheological characterization of microfibrillated cellulose suspensions after freezing. Carbohydrate Polymers, 80(3), 677-686.
- Albornoz-Palma, G., Betancourt, F., Mendonça, R. T., Chinga-Carrasco, G., & Pereira, M. (2020). Relationship between rheological and morphological characteristics of cellulose nanofibrils in dilute dispersions. *Carbohydrate polymers*, *230*, 115588.
- Grüneberger, F., Künniger, T., Zimmermann, T., & Arnold, M. (2014). Rheology of nanofibrillated cellulose/acrylate systems for coating applications. Cellulose, 21(3), 1313-1326.
- Iotti, M., Gregersen, Ø. W., Moe, S., & Lenes, M. (2011). Rheological studies of microfibrillar cellulose water dispersions. Journal of Polymers and the Environment, 19(1), 137-145.
- Iwamoto, S., Lee, S. H., & Endo, T. (2014). Relationship between aspect ratio and suspension viscosity of wood cellulose nanofibers. Polymer journal, 46(1), 73-76.
- Mansfield, M. L., & Douglas, J. F. (2008a). Transport properties of rodlike particles. Macromolecules, 41(14), 5422–5432. https://doi.org/10.1021/ma702839w
- Mansfield, M. L., & Douglas, J. F. (2008b). Transport properties of wormlike chains with applications to double helical DNA and Pääkkö, M., Ankerfors, M., Kosonen, H., Nykänen, A., Ahola, S., Österberg, M., \& Lindström, T. (2007). Enzymatic hydrolysis combined with mechanical shearing and high-pressure homogenization for nanoscale cellulose fibrils and strong gels. Biomacromolecules, 8(6), 1934-1941.
- Tanaka, R., Saito, T., Ishii, D., \& Isogai, A. (2014). Determination of nanocellulose fibril length by shear viscosity measurement. Cellulose, 21(3), 1581-1589.
- Wang, Q. Q., Zhu, J. Y., Gleisner, R., Kuster, T. A., Baxa, U., \& McNeil, S. E. (2012). Morphological development of cellulose fibrils of a bleached eucalyptus pulp by mechanical fibrillation. Cellulose, 19(5), 1631-1643.

Effect of the morphological characteristics and size distribution on the rheological properties of Cellulose Nanofibrils dispersions

Gregory Albornoz-Palma, Daniel Ching, and Miguel Pereira

Department of Chemical Engineering
Engineering Faculty
Universidad de Concepción